



HAL
open science

A deterioration-aware energy management strategy for the lifetime improvement of a multi-stack fuel cell system subject to a random dynamic load

Jian Zuo, Catherine Cadet, Zhongliang Li, Christophe Bérenguer, Rachid Outbib

► To cite this version:

Jian Zuo, Catherine Cadet, Zhongliang Li, Christophe Bérenguer, Rachid Outbib. A deterioration-aware energy management strategy for the lifetime improvement of a multi-stack fuel cell system subject to a random dynamic load. *Reliability Engineering and System Safety*, 2024, 241 (January 2024), pp.109660 (17). 10.1016/j.ress.2023.109660 . hal-04257440v2

HAL Id: hal-04257440

<https://hal.science/hal-04257440v2>

Submitted on 25 Oct 2023

HAL is a multi-disciplinary open access archive for the deposit and dissemination of scientific research documents, whether they are published or not. The documents may come from teaching and research institutions in France or abroad, or from public or private research centers.

L'archive ouverte pluridisciplinaire **HAL**, est destinée au dépôt et à la diffusion de documents scientifiques de niveau recherche, publiés ou non, émanant des établissements d'enseignement et de recherche français ou étrangers, des laboratoires publics ou privés.

Highlights

A deterioration-aware energy management strategy for the lifetime improvement of a multi-stack fuel cell system subject to a random dynamic load

Jian Zuo, Catherine Cadet, Zhongliang Li, Christophe Bérenguer, Rachid Outbib

- Stochastic deterioration model with load-dependent and stack-to-stack variability
- Multi-stack fuel cell system operating under random dynamic load profiles
- Proposition of a deterioration aware energy management strategy
- Joint management of load allocation and switching decisions for multi-stack fuel cells

A deterioration-aware energy management strategy for the lifetime improvement of a multi-stack fuel cell system subject to a random dynamic load

Jian Zuo^{a,b,c}, Catherine Cadet^a, Zhongliang Li^{b,*}, Christophe Bérenguer^a, Rachid Outbib^c

^aUniv. Grenoble Alpes, CNRS, Grenoble INP, GIPSA-lab, Grenoble, 38000, France

^bUniversité de Franche-Comté, UTBM, CNRS, Institut FEMTO-ST, 90000, Belfort, France

^cLIS Laboratory, Aix-Marseille University, Marseille, 13397, France

Abstract

Proton exchange membrane (PEM) fuel cells still suffer from the challenge of limited durability, hindering their widespread commercialization. To overcome this limitation, resorting to Multi-stack Fuel Cell (MFC) systems instead of single fuel cells is a promising solution. Indeed, by optimally distributing the power demand among the different stacks while taking into account their state of health, an efficient Energy Management Strategy (EMS) can be achieved. Here a new multi-stack configuration, based on an oversized multi-stack system is explored. The problem addressed in this paper is to develop a methodology that manages the operation of an oversized three-stack system where only two of them operate simultaneously. The first stage is to predict the deterioration rate of each stack according to the load allocation, and link the deterioration rate of each stack with the load dynamics. To that end, several stochastic deterioration models, from the classical Gamma process model to more complex models with random effects have been developed and tailored to the fuel cell specificities. Then, an event-based decision-making strategy has been established, that determines the load allocations among the operating stacks. This strategy is based on the minimization of the deterioration phenomena due to both the load amplitude and the load variations. Finally, this strategy is extended to the three-stack oversized system by adding the decision to start or stop a stack. These strategies have been validated under random dynamic load profiles, and Monte Carlo simulation results verify the efficiency of the proposed strategies through improved system lifetime.

Keywords: Multi-stack fuel cells, stochastic deterioration, random dynamic load profile, health-aware energy management strategies

1. Introduction

1.1. Background

Nowadays, the severe climate change challenges caused by the wide use of fossil fuel stimulates the need of developing clean power sources to increase the usage of clean fuels. PEM fuel cell is one of these power sources which uses hydrogen and oxygen to produce electricity, with products of water and heat. Thanks to their relatively high power density, suitable operation temperature, and easy scale-up, PEM fuel cells have been applied to various applications, including transport applications. However, the current PEM fuel cell technology has not achieved widespread commercialization due to its limited durability.

Prognostics and health management (PHM) is one solution to solve the fuel cell durability challenge [1]. PHM is a systematic approach that can deal with system assessment, diagnostics, prognostics, and decision-making support [2]. Fuel cell diagnostics is targeted to identify system degradation levels, raise alarms in the case of faulty operation modes, and analyze the main factors for fuel cell fault operation [3]. Prognostics deals with the prediction of fuel

*Corresponding author.

Email addresses: jian.zuo@utbm.fr (Jian Zuo), catherine.cadet@grenoble-inp.fr (Catherine Cadet), zhongliang.li@univ-fcomte.fr (Zhongliang Li), christophe.berenguer@grenoble-inp.fr (Christophe Bérenguer), Rachid.Outbib@lis-lab.fr (Rachid Outbib)

cell future deterioration trends and finally obtaining the remaining time to reach a pre-defined failure threshold, that is, remaining useful lifetime [4]. However, though fuel cell diagnostic and prognostic methods have been extensively developed, only few of them have been used as decision-making support to improve fuel cell durability. An efficient decision can be to adapt the energy demand to the health state of the fuel cell, which can be achieved within an energy management strategy (EMS).

Most of the studies in this domain have been developed for hybrid fuel cell systems, which are broadly composed of a single fuel cell and a battery. For these systems [5], the energy management strategies handle several objectives that mainly include i) satisfying system power demand; ii) improving fuel economy and system efficiency; iii) enhancing the lifetime of fuel cells.

The deterioration-aware EMSs deal with improving fuel economy while considering deterioration. Recent studies [6, 7, 8, 9] emphasized the need to develop deterioration-aware EMSs mainly for two reasons. First, the primary challenge of current fuel cells is their limited durability which has to be handled through the management of fuel cell deterioration. Moreover, ignoring the performance decay of a fuel cell may increase system fuel consumption, resulting in a low fuel economy. Developing a deterioration-aware EMS is generally treated as an optimization problem in which the fuel cell degradation is modeled in order to be integrated into the optimization process. De Pascali et al. [10] proposed a deterioration-aware EMS for hybrid vehicles by incorporating the electrochemical degradation dynamics of the battery, thus improving system lifetime and achieving fuel economy. A deterioration-aware energy management approach is proposed in [11] to deal with lifetime improvement of ship hybrid plants. The proposed strategy considers the tradeoff operation between fuel consumption and system degradation, achieving a 4 times reduction in system failure rate. Peng et al. [12] proposed a hierarchical management strategy for enhancing system fuel economy and durability of a heavy-duty hybrid power system. However, there is no explicit degradation model for fuel cell deterioration. Speed prediction-based EMS for fuel cell electric vehicles (FCEVs) is presented by Zhang et al. [13]. The fuel cell economy and power train system durability are modeled through a mathematical model and directly used to formulate the optimization objective functions. The formulated optimization problem is solved by using a sequential quadratic programming method.

Additionally, some strategies include maintenance costs (e.g., fuel cell replacement cost) and are referred to as maintenance-based EMSs. The combination of managing fuel cell deterioration and system reliability as well as maintenance costs enables the development of a more durable and reliable fuel cell system. The definition of maintenance, according to the standard (IEV 192-06-01), is the combination of all technical and management actions during the life cycle of an item intended to retain the item in, or restore it to, a state in which it can perform as required [14]. Unfortunately, few works are available on this topic in the field of fuel cell systems. Vasilyev et al. [15] proposed a dynamic reliability model for a single fuel cell system. However, they did not develop a management strategy for improving the fuel cell system lifetime. Gargari et al. [16] proposed a preventive maintenance scheduling strategy for a multi-energy microgrid. The validation on three operation scenarios confirms that the proposed maintenance strategy achieved 30% reliability improvement on average.

The aforementioned works are focused on the context of hybrid fuel cell systems with a single fuel cell stack. However, there is a growing need for high-power capacity in the current fuel cell market. Thereby, current fuel cell EMS studies are expected to be adapted for this requirement. Among solutions, multi-stack fuel cell (MFC) systems, composed of multiple stacks, are promising.

1.2. Energy management strategies for multi-stack fuel cell systems

A MFC system is composed of several stacks, either in series or in parallel architecture [17]. In a series configuration, the system output voltage is the summation of individual stack voltage, while for parallel architecture, the DC/DC converters connected to the stacks share the same level of output voltage. The parallel configuration is preferred because of its efficiency in minimizing the fuel cell system deterioration [18]. The integration of multiple stacks enables them to provide higher power. Thanks to the modular architecture, MFC systems offer a number of strengths compared to the single stack configuration. Firstly, MFC systems offer more redundancy than a single stack and thus the system reliability is improved. Another one is that the durability of MFC systems can be increased by optimally distributing the power demand among different stacks. In addition, as MFC can be manufactured in standard size and can be easily combined to meet different power demands, this could help balance the increased cost of modular architecture [19]. In short, MFC systems are relevant to meet this challenge if properly dimensioned and managed by an appropriate EMS taking into account the deterioration of the stacks.

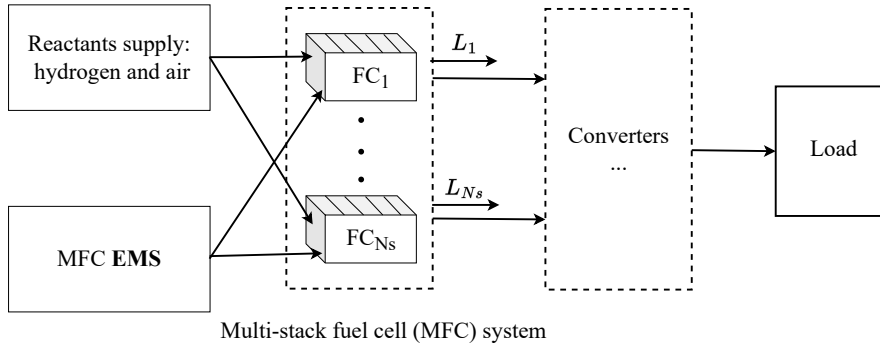


Figure 1: Schematic of multi-stack fuel cell system operation principle.

Figure 1 depicts the overall scheme of a multi-stack fuel cell system and its operation principle. In general, the EMS block is designed to decide the load allocation between different stacks to provide the required power demand. The main focus is how to extend the MFC system lifetime through an optimized load allocation at each decision time step. According to the studies of the single-stack fuel cell systems, the basic, deterioration-aware, and maintenance-based EMS can be extended to the study of MFC systems. Several works studied the optimization-based EMS for minimizing MFC fuel consumption. Wang et al. [20] proposed a forgetting factor recursive least square algorithm-based EMS to improve parallel-connected MFC system efficiency and reduce fuel consumption. The FFRLS algorithm ensures an accurate estimation of MFC system parameters which is suitable for online power allocation. The efficiency of the proposed strategy is validated with a two-stack 300 W PEM fuel cell system. Moghadari et al. [21] built an equivalent fuel consumption minimization strategy for a MFC system. The results showed that the proposed energy management strategy achieved a similar consumption as the Dynamic Programming method, although it is an online optimization strategy. Several sophisticated designs of EMSs have been proposed recently. Wang et al. [22] have developed a two-level EMS to improve fuel cell system operation efficiency. For the considered hybrid power system consisting MFCs and batteries, the first level of EMS is designed to manage the operation of MFC, and the second level is on the coordination of fuel cell and battery. The overall MFC system performance is improved through the proposed strategy.

Then the deterioration-aware EMS is developed for MFC systems to address the durability issue. Ghaderi et al. [23] designed a two-layer EMS for a MFC system-based FCEV. The first layer is responsible for estimating the system health state, i.e., fuel cell maximum power and maximum efficiency points. Then based on this information, a second layer is developed to build the strategy that optimizes the operation loads between different power sources. This two-layer EMS can effectively minimize system fuel consumption and power source deterioration through optimized load allocations. Fernandez et al. [24] further proposed an adaptive state machine-based approach for improving MFC system durability and fuel economy. The first layer is composed of an empirical fuel cell deterioration model and a Kalman filter which is used to estimate deterioration parameters. The second layer makes the decision on the allocation of the operating load for each stack. The effect of the proposed strategy is verified by comparison with the Average Load and Daisy Chain strategies. However, in the above studies, fuel cell deterioration is only modeled as a function of time and no direct links between fuel cell deterioration and their influence factors are considered. A few research works have recently emerged to address this issue. Herr et al. [25] proposed an empirical deterioration model by linking the fuel cell's remaining useful lifetime with the operating power. Then a post-prognostic decision strategy is proposed based on this model to improve fuel cell lifetime. A mix integer programming method is used to solve the decision-making problem, deciding the optimal operation load for each stack. Based on a similar deterioration modeling approach, Zhou et al. [26] extended the load allocation strategy by adding the minimization of system fuel consumption. Moreover, a stochastic dynamic load demand profile adapted from the world transition vehicle cycle is used as the application scenario. The optimal load allocations are obtained by solving a bi-level optimization problem with remaining useful lifetime (RUL) and efficiency as the objective functions. Bankati et al. [27] improved fuel cell deterioration model by integrating calendar aging and operation cycling aging. Then, an online RUL-based EMS is developed for a MFC system to minimize system fuel consumption and deterioration, obtaining 30% improved

lifetime compared to the classic average load split method.

Few studies have been conducted to address the development of strategies considering maintenance cost optimization. Colombo et al. [28] performed a reliability analysis of a MFC system with strict constant power supply requirements. The system failure probability function is built based on the experimental data and physics-based deterioration model. Reliability analysis of a MFC from a system engineering perspective is presented by Colombo and Kharton [29]. They systematically demonstrate the methodology of combining physical modeling and experimental data to construct system failure probability which is inspiring for fuel cell-based system reliability studies. Based on the results of reliability analysis, maintenance studies are performed to further enhance the reliability and durability of MFC systems. Phommixay et al. [30] applied preventive maintenance (PM) to combine with the power-sharing of different power sources to study the operation of a MFC-based microgrid system. The optimization objective of the microgrid system is composed of finding the lowest total operation cost while meeting the load requirements as well as the physical constraints of power sources. The PM is implemented to prevent system breakdown.

1.3. Identified research gaps and contributions

Considering the research works cited above, the following knowledge gaps in the energy management of fuel cell systems are identified as:

1. *Modular architecture exploitation.* The majority of available EMSs are developed for hybrid fuel cell systems that focus on the battery state of charge and neglect the fuel cell aspects. Thus, the advantages of the flexibility offered by the modular architecture of a MFC remain unexplored.
2. *Fuel cell deterioration handling.* The degradation behavior of PEM fuel cells is extremely complex. It encompasses a series of mechanical, chemical, and electrochemical processes. However, as MFC deterioration rate is also closely linked to its operation load, a model linking them is required.
3. *Maintenance cost handling.* The maintenance cost of MFC is related to system reliability and stack replacement. Thus, integrating the optimization of maintenance cost for MFC is required in practice. Nearly no work is being done in terms of the MFC system.

Considering these gaps, the following contributions are made in this paper:

- An empirical deterioration rate formula is integrated into a Gamma process-based deterioration model for MFC system to take into account load dependency and stack-to-stack deterioration variability.
- An efficient energy management based on a stochastic deterioration model is proposed to deal with the dynamic random load.
- A switching approach is developed for an oversized MFC system to further enhance the system lifetime of the MFC system.
- The start and stop of stacks are handled which opens the way to a maintenance approach.

1.4. Multi-stack fuel cell management problem statement

Multi-stack fuel cell system configuration. Let M_{N_s} denote a MFC system with N_s parallel-connected stacks. All the individual stacks are assumed to be manufactured with the same production capacity with output power ranges from minimal power L_{min} to maximal power L_{max} . One important issue for fuel cell systems is their performance decay which is the main focus of this work. The overall deterioration of fuel cells can be attributed to mechanical, electrochemical, and thermal sources which are closely linked to fuel cell operation load modes and operation parameters.

Energy management problem. Figure 2 shows the overall energy management problem of an oversized multi-stack system ($N_s = 3$). The oversized multi-stack fuel cell system refers to a system consisting of more stacks than necessary to supply the max requested load, which allows to stop (at least) one stack. The overall system production demand is defined by a dynamic load cycle, as depicted in the figure. The MFC system has three individual stacks, only two of which are operating at the same time to provide the required power demand. Two levels of decisions are needed to support the system operation, i.e., the stack switching decision, and the load allocation decision for operating stacks. Then, the energy management problem can be divided into two sub-problems.

2.2. Proposed Gamma process-based stochastic deterioration models

The deterioration of a fuel cell, according to Pei et al. [35], is broadly divided into start-stop cycling, load change cycling, idling, and high power load conditions. We adapted these deterioration factors as deterioration due to load amplitude, to load variation, and to start-stop cycling, expressed as:

$$\Delta R = \Delta R_L + \Delta R_{\Delta L} + \Delta R_{ss} \quad (1)$$

where ΔR is the overall deterioration of fuel cell stack resistance. ΔR_L is the resistance deterioration increment caused by the load-dependent intrinsic deterioration phenomenon, $\Delta R_{\Delta L}$ is the load variation caused deterioration, and ΔR_{ss} stands for the start-stop operation deterioration.

The health indicator is derived from a widely adopted empirical polarization equation developed by Kim et al. [31]. The static performance model is expressed as:

$$E_s = n_{cell} (E_{rev} - A \log(I) - RI - m \exp(nI)) \quad (2)$$

where I is fuel cell current density. E_s is stack output voltage, n_{cell} is the number of cells in a stack. E_{rev} is the reversible voltage. The activation losses are expressed by $A \log(I)$, A is the Tafel parameter for oxygen reduction. R is the resistance. The concentration (mass transfer) losses are calculated by $m \exp(nI)$. m and n are transfer coefficient-related parameters. Thus, Eq. (2) involves only resistance and not a total impedance (capacitance and inductance are excluded here).

According to fuel cell literature [35], the load variation and start-stop event caused system deteriorations are modeled as deterministic quantities, whereas ΔR_L is a stochastic quantity.

Modelling the $\Delta R_{\Delta L}$ and ΔR_{ss} deterioration factors. The load variation caused deterioration $\Delta R_{\Delta L}$ is given by

$$\Delta R_{\Delta L} = K \Delta L \quad (3)$$

where coefficient K ($\Omega.cm^2 / W.cm^{-2}$) is calculated using a reference value, as

$$K = \frac{K_{\Delta R} D_{R,\Delta R}}{L_{max} - L_{min}} \quad (4)$$

where $D_{R,\Delta R}$ ($\Omega.cm^2 / W.cm^{-2}$) is a reference deterioration rate by load variation adapted from Pei et al. [35], and $K_{\Delta R}$ is considered a constant corresponding to the specific fuel cell technology.

The start-stop operation deterioration factor is given by

$$\Delta R_{ss} = R_0 D_{ss} \quad (5)$$

where R_0 is the initial resistance of a fuel cell. D_{ss} stands for resistance deterioration rate due to one start and stop event.

Homogeneous Gamma process deterioration model for ΔR_L . The dynamic evolution of the resistance deterioration caused by the load-dependent intrinsic deterioration phenomenon is assumed to be continuous and it is modeled by a stochastic process to account for its variability. It is assumed that under constant load, the degradation phenomenon is homogeneous in time in the sense that the fuel cell degradation growth rate remains constant over time, and thus the degradation increments on disjoint time intervals are independent one to each other, and depend only on the interval duration. Such a degradation phenomenon can be modeled using a homogeneous Gamma process. A Gamma process is a stochastic process with independent, positive increments that obey a Gamma distribution $Ga(\nu, \beta)$ characterized by two key parameters: its shape parameter ν and scale parameter β [36, 37, 38]. By definition, the load amplitude caused increment of fuel cell resistance ΔR_L between time t_1 and t_2 ($t_2 > t_1 \geq 0$) is given by:

$$\Delta R_L(t_1, t_2) \sim Ga(\nu(t_2 - t_1), \beta) \quad (6)$$

where $\Delta R_L(t_1, t_2) \triangleq R_L(t_2) - R_L(t_1)$. $Ga(\nu(t_2 - t_1), \beta)$ represents the probability density function of the Gamma law with shape function $\alpha(t)$ and scale parameter β :

$$f_{Ga}(x, \nu(t_2 - t_1), \beta) = \frac{x^{\nu(t_2 - t_1) - 1} e^{-x/\beta}}{\beta^{\nu(t_2 - t_1)} \Gamma(\nu(t_2 - t_1))} \quad (7)$$

where $\Gamma(t) = \int_0^{+\infty} x^{t-1} e^{-x} dx$ is the Gamma function.

It can be noted that using a Gamma process is not the only possible choice for stochastic deterioration modeling for fuel cells. The deterioration could have been modeled by another stochastic process, such as inverse Gaussian or Wiener, without changing essentially our methodological proposition: the important point here is to have at one's disposal a model accounting for the dynamic of the degradation and its link to the operating load in order to predict its evolution, and adapted to the observed data.

The use of a Gamma process can be further justified [34]:

- From a methodological point of view, a Gamma process is particularly suitable to model monotonic continuous increasing deterioration that accumulates over time through many tiny increments. The deterioration of fuel cell resistance follows such a degradation trend;
- Furthermore, from a practical point of view, a good fit has been observed between the modeled resistance deterioration using GP and the experimental observations, [34, 33];
- In addition, Gamma process exhibits some nice mathematical properties, that make it a tractable modeling tool: a gamma-distributed increment observed on different durations still obeys a gamma law, which makes it suitable for modeling various phenomena.

Load-dependent modelling. To account for the effect of the varying load on the degradation growth rate, the law of the degradation increment at a given time (and hence of the Gamma process shape parameter) is made dependent on the load, and the degradation growth rate becomes a function of the load applied to the fuel cell, which leads to considering a non-homogeneous degradation Gamma process, driven by the load process. To link fuel cell deterioration with operation load, i.e., load dependency, an empirical deterioration rate function ($D(L)$) is proposed for the Gamma process model. The shape parameter ν is modeled as a function of the load L . The mean of resistance increment over a time unit interval, which is also the average deterioration rate, can thus be written as:

$$D(L) = \nu(L)\beta \quad (8)$$

Figure 3 shows the proposed parabola shape deterioration curves. As seen from the figure, the lowest deterioration rate is assigned to the nominal load, whereas the minimal load and maximal load conditions are exposed to higher deterioration rates. The deterioration rate function $D(L)$ is formulated as

$$D(L) = A(L - L_{nom})^2 + B \quad (9)$$

where A is expressed by two parts with respect to the load range, i.e. $A = A_1, L_{min} \leq L < L_{nom}$ and $A = A_2, L_{nom} \leq L \leq L_{max}$. Then the deterioration model changes into a non-homogeneous Gamma process to adapt for the load dependency characteristic. More details of the development of this deterioration curve refer to [33].

Random-effects Gamma process models for ΔR_L . The deterioration in different fuel cell stacks has a large variation due to some hidden effects. That is, fuel cell stack deterioration is not only influenced by operating load, but also due to some random effects which will cause deterioration variability among different stacks. And the standard GP model is unable to fully capture such variations, i.e., individual deterioration heterogeneity. One of the approaches to integrate the unobserved random effects is to make one or more model parameters unit-specific when the Gamma process is applied. On this basis, we propose a GP model with random effects for modeling MFC system deterioration. A random effect is imposed on the scale parameter, which is taken as a random variable following a Gamma distribution [39]. Each individual fuel cell stack corresponds to one realization of the random parameter. More precisely, three different types of random effects-based models are investigated, namely, the Gamma process random-effect model

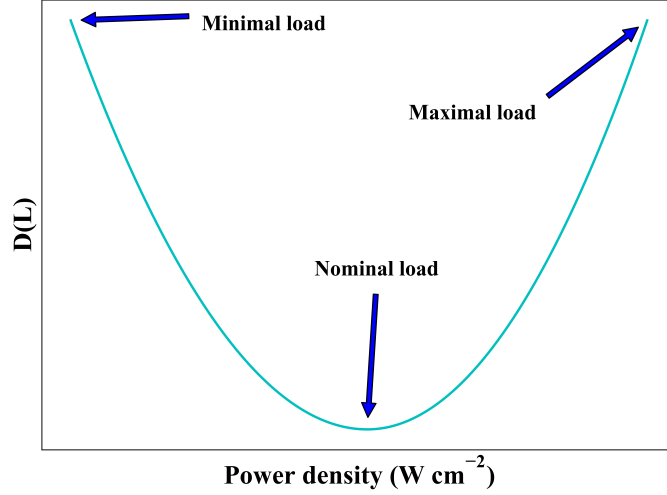


Figure 3: Dependence of fuel cell deterioration rate (overall resistance) on power load demand

(GP-RE), Gamma process random mean model (GP-RM), and Gamma process random variance model (GP-RV). The GP-RE model is expressed as:

$$\begin{aligned}\Delta R_L(t_1, t_2) &\sim Ga(v \cdot (t_2 - t_1), \beta_s) \\ \beta_s &\sim Ga(\delta, \phi)\end{aligned}\quad (10)$$

where δ, ϕ are the shape and scale parameter that formulates the gamma distribution for β in the standard GP model. The new shape parameter sampled from $Ga(\delta, \phi)$ is denoted as β_s .

This model is called the GP-RE model. The mean and variance of the GP-RE model in the time interval $(t_1, t_2), t_2 > t_1 \geq 0$ is calculated as:

$$\begin{aligned}\text{Mean}(\Delta R_L(t_1, t_2)) &= v \cdot (t_2 - t_1) \cdot \beta_s \\ \text{Var}(\Delta R_L(t_1, t_2)) &= v \cdot (t_2 - t_1) \cdot \beta_s^2\end{aligned}\quad (11)$$

Since the random effects for all models are added through Gamma law, one basic principle here is to keep the mean value ($\delta\phi$) equal to the original scale parameter β (denoted as β_0). In the above three random-effect models, the scale parameter of standard GP follows a Gamma distribution, and it is unit-specific, such that it can capture the individual deterioration variability. More details on the remaining random-effects models can be found in [34].

Now that we have built the stochastic load-dependent deterioration models for the MFC system, the next step is to develop an energy management strategy for the formulated MFC management problem.

3. Energy management strategies

This section presents the proposed EMS for managing the operation of an oversized MFC system. This EMS aims at driving both the switching between stacks and the load allocation among them. These two decisions (switching and load allocation) are optimized by considering two decision criteria that are linked to the MFC deterioration, such that an extended system lifetime can be achieved. In this section, we consider a MFC system with N_s stacks, among which n are operated and $N_s - n$ are kept stopped; n is kept constant for all the decision periods.

Specifically, a two-step decision-making strategy is developed. Firstly, an EMS rule is developed to decide the load allocation for any combination of n operating stacks. Then, a second EMS decision rule is built which focuses on the stacks switching by selecting the combination of the operating stack that minimizes the future MFC deterioration.

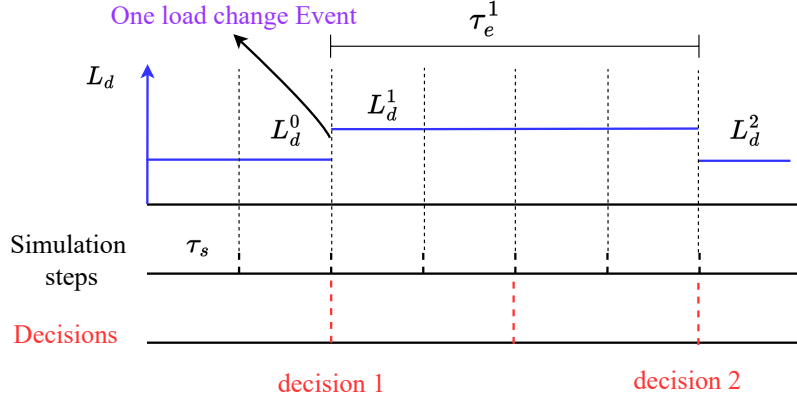


Figure 4: Event-based decisions under a dynamic load profile

3.1. EMS rule for the load allocation on operating stacks

Considering the dynamic load profile, a load change event-based decision-making procedure is applied as introduced in Figure 4. A new load allocation decision is triggered whenever a load change event is detected. For instance, at decision 1, a change in load demand level is detected and the allocated loads are changed from L_d^0 to L_d^1 .

Figure 5 presents the decision-making principle in presence of dynamic loads (with n operating stacks). The decision process is conducted whenever a load level change event is detected. At decision time “1”, a load allocation decision is made for the following $j = 2, \dots, m$ events. Then, the deterioration level of each of the n stacks caused by load amplitude and load variation is estimated based on the proposed deterioration model (Equation (1)) over the considered load change events history. And finally, the decision-making strategy allocates the loads by selecting the allocation pattern that leads to the lowest estimated deterioration.

The duration between load change events is considered to be random. At the decision stage, it can either be known (requested from fuel cell operator or predicted with high-cost estimation techniques) or be unknown. The influence of the knowledge of this duration on the performance load allocation decision strategy is investigated in Section 4.4. When the event duration is unknown, an expected event duration ($\bar{\tau}_e$) estimated from the MC model is used in the decision-making process (Equation (A.4)).

Optimization problem. Denoting γ_i^j the load allocation ratio for FC i at decision time j ($j = 1, \dots, m$), and according to the above-described decision-making principle, the load allocation strategy can be formalized as a constrained nonlinear optimization problem:

$$\begin{aligned}
& \underset{\{\gamma_i^j\}_{i=1, \dots, n}}{\text{minimize}} && J_{dec1}(\{\gamma_i^j\}_{i=1, \dots, n}) = \sum_{i=1}^n \omega_i \left\{ \sum_{j=1}^m \left(\Delta R_{L,i}^j + (\Delta R_{\Delta L,i}^j)^2 \right) \right\} \\
& \text{subject to} && L_{min} \leq \gamma_i^j L_d^j \leq L_{max}, \sum_{i=1}^n \gamma_i^j = 1, \quad j = 1, \dots, m \\
& && \Delta R_{L,i}^j = D(\gamma_i^j L_d^j) \cdot \tau_e^j, \quad j = 1, \dots, m \\
& && \Delta R_{\Delta L,i}^1 = K |\gamma_i^1 L_d^1 - \gamma_i^0 L_d^0| \\
& && \Delta R_{\Delta L,i}^j = \sum_{j=2}^m K |\gamma_i^j L_d^j - \gamma_i^{j-1} L_d^{j-1}|, \quad j = 2, \dots, m
\end{aligned} \tag{12}$$

where τ_e^j is the time length of event j , m is the number of future events taken into account during each decision (i.e., the decision horizon), the index “1” refers to the current load change event, and the index “0” refers to the previous load change event. L_d^j defines the external dynamic load demands. The distance of the deterioration level R_{FCi}^0 of the fuel cell FC i to the preset failure threshold FT is leveraged to formulate the weight factor ω_i for fuel cell FC i :

$$\omega_i = \frac{1/(FT - R_{FCi}^0)}{\sum_{i=1}^n 1/(FT - R_{FCi}^0)} \tag{13}$$

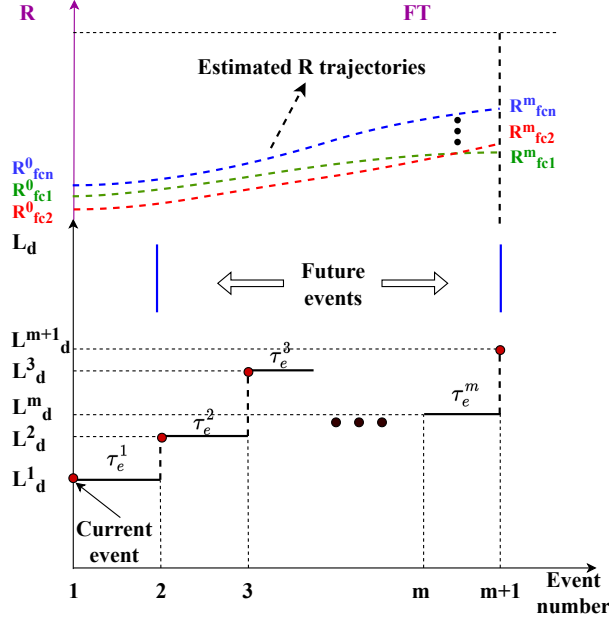


Figure 5: Principle of the proposed decision procedure.

3.2. EMS rule for stacks switching decisions

The switch decisions can then be optimized based on the previously developed load allocation strategy. For a MFC system, several combinations of operating stacks (with the previously determined load allocations) can be considered which correspond to different switching decisions. Thus, a decision criterion is needed to make the optimal decision among all possible operating stacks combinations. This is implemented by the following two steps.

- Step 1: Deciding the load allocations for all possible operating stacks combinations.

Considering a MFC system with N_s stacks, there are $\binom{N_s}{n}$ possible combinations for operating n stacks and keeping $N_s - n$ stacks stopped ($n \leq N_s$, and n is assumed to remain the same at each decision step). For example, for a three stacks problem with two operating stacks ($N_s = 3, n = 2$), the possible combinations are listed as

$$\begin{aligned}
 comb_1 &= \{FC_{op1} = FC1, FC_{op2} = FC2, FC_{st} = FC3\} \\
 comb_2 &= \{FC_{op1} = FC1, FC_{op2} = FC3, FC_{st} = FC2\} \\
 comb_3 &= \{FC_{op1} = FC2, FC_{op2} = FC3, FC_{st} = FC1\}
 \end{aligned} \tag{14}$$

where FC_{op1}, FC_{op2} are the two operating stacks, and FC_{st} is the stopped stack. Then, for each combination of operating stacks, the load allocation decision is optimized by solving the optimization problem as defined in Equation (12) (J_{dec1}), which gives the load allocation ratios $\{\gamma_i^j\}_{i=1, \dots, n}$ (note that here γ_i is the allocation ratio decision for the operating stack i after renumbering the operating stacks from 1 to n).

- Step 2: Selecting the optimal combination of operating stacks

In order to select the optimal combination of operating stacks, a second deterioration criterion J_{dec2} integrating the system deterioration evolution incurred by each combination has to be computed. For each combination $comb_j$, the stacks can be categorized into four groups based on the deterioration that they will suffer from being inserted (or not) in this combination at the considered decision time j :

- 1) $G1_{comb_j}$: this group includes all the stacks that were operating and are kept operating in the combination $comb_j$ selected at the current decision time. The expected cumulative group deterioration $Det_{comb_j}^{G1}$ is caused by the load variation and load magnitude deterioration factors.

- 2) $G2_{comb_j}$: this group includes all the stacks that were operating and are stopped in the combination $comb_j$ selected at the current decision time. The group deterioration $Det_{comb_j}^{G2}$ equals zero.
- 3) $G3_{comb_j}$: this group includes all the stacks that were stopped and are started in the combination $comb_j$ selected at the current decision time. The group deterioration $Det_{comb_j}^{G3}$ is caused by load magnitude and start-stop factors.
- 4) $G4_{comb_j}$: this group includes all the stacks that were stopped and are kept stopped in the combination $comb_j$ selected at the current decision time. The group deterioration $Det_{comb_j}^{G4}$ equals zero.

Hence, the decision criterion J_{dec2} can be expressed as

$$\begin{aligned}
J_{dec2}(\{comb_j\}_{j=1,\dots,m}) &= \sum_{j=1}^m Det_{comb_j}^{G1} + Det_{comb_j}^{G2} + Det_{comb_j}^{G3} + Det_{comb_j}^{G4} \\
&= \sum_{j=1}^m Det_{comb_j}^{G1} + Det_{comb_j}^{G3}
\end{aligned} \tag{15}$$

In Equation (15), for the term $Det_{comb_j}^{G3}$, the contribution due to the deterioration incurred by one start-stop cycle ($\Delta R'_{ss}$) is calculated as

$$\Delta R'_{ss} = k_{ss} \Delta R_{ss} \tag{16}$$

where k_{ss} is a hyper-parameter to be optimized, which is related to the fuel cell failure threshold (FT):

$$k_{ss} = \begin{cases} k_1 & \text{if } 0.9FT \leq \max_{k=1,\dots,N_s}(R_{FC_k}) \\ k_2 & \text{else} \end{cases} \tag{17}$$

k_1 and k_2 are two parameters for fuel cell stack at different deterioration levels. When the maximum resistance among the N_s stacks reaches 90% of the failure threshold, the start-stop deterioration cost term is quantified by k_1 . For a maximum resistance level below this threshold ($0.9FT$), the start-stop deterioration cost term is quantified by k_2 . These weighting parameters k_1 and k_2 are linked with the optimization of switching decisions. When this weight is small, the cost of switching on/off stacks is relatively low, thus increasing the frequency of start and stop actions. On the contrary, when the weight is large, the frequency of start-stop action will be decreased due to the high cost of switching on/off stacks. Thus, here k_1, k_2 satisfy $k_2 < k_1$.

The final optimal combination of the operating stacks is then obtained by solving the following problem

$$\underset{\{comb_j\}_{j=1,\dots,m}}{\text{minimize}} \{J_{dec2}(\{comb_j\}_{j=1,\dots,m})\} \tag{18}$$

where J_{dec2} is the second deterioration criteria as defined in Equation (15). The optimized combination of operating stacks and its corresponding load allocation solved at decision step 1 in Equation (12) give the final decision of the proposed decision-making strategy.

In the following, we will consider only the case of a decision horizon of length one, i.e. $m = 1$, which means that only the period until the next change load event is considered.

3.3. Application to a three-stack system

Figure 6 depicts the proposed operation strategy for a three-stack operation EMS problem, with $N_s = 3, n = 2$. At the beginning of system operation, three stacks are available for operating (no stack failure occurs). Then the above two-step optimization is applied to select the two operating stacks and optimal load allocation for these two stacks. In the diagram, this two-step optimization is represented by J_{dec1} for deciding the optimal load allocations for all possible operation combinations, and the switch decision is optimized through J_{dec2} . When the system deteriorates to a certain level, stack failure may happen for the studied MFC system. When only one stack fails, the remaining two stacks keep running to provide the power demand. At this stage, there is no choice of replacing stacks, the strategy only optimizes the load allocation between these two stacks. And finally, the system failure is triggered by the time when two stacks fail.

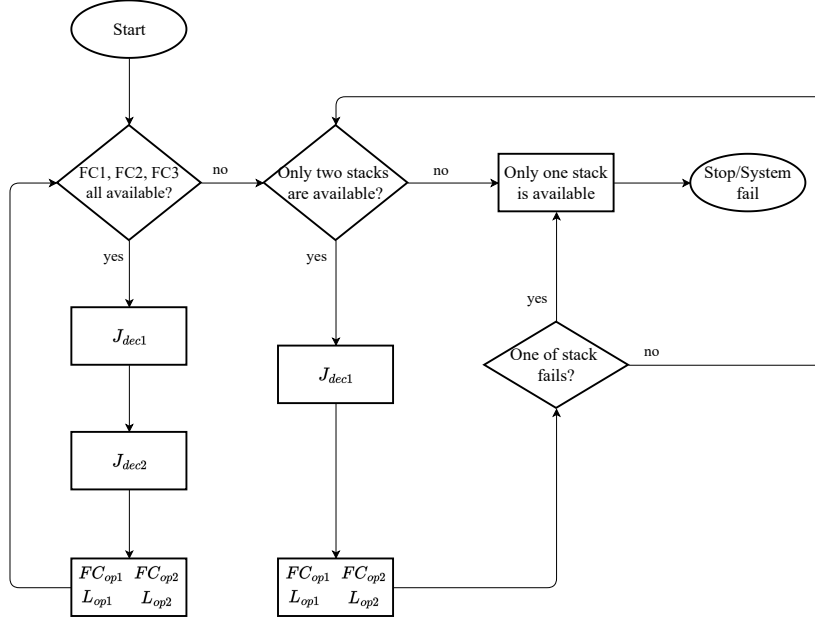


Figure 6: Diagram of the proposed two-step decision-making strategy.

4. Simulation results and discussion

4.1. Simulation settings

Main simulation parameters. Table 1 lists the main simulation parameters, taken from [40]. Fuel cell stack output powers ($L_{min}, L_{nom}, L_{max}$), expected stack lifetimes ($\bar{T}_{R,min}, \bar{T}_{R,nom}, \bar{T}_{R,max}$), and initial resistance (R_0) are the main parameters for fuel cell stack basic physical parameters. The maximum output power L_{max} is set as a fixed physical parameter based on the initial fuel cell stack design. In our simulation, we consider that the stacks can supply the same amount of power even at the end of their lifetime. To obtain the necessary prior knowledge, such as the expected lifetime, experimental investigation work is required to test the degradation rate and subsequently estimate the stack's lifetime. This information is then taken into account in the proposed deterioration model. Additionally, as the stacks are supposed to be identical, the fresh stacks have the same model.

The shape parameter (v), scale parameter (β_0), and failure threshold (FT) are the main parameters of fuel cell stack deterioration models. The fuel cell physical parameters are taken from a fuel cell experimental dataset [41]. The maximum output power of the studied three-stack fuel cell is computed as 1.16 kW. The shape and scale parameters are estimated from the same dataset, using the method of moments approach.

Besides the parameters specific to fuel cells, the hyper-parameters k_1 and k_2 shown in Equation (17) are selected based on the grid search results presented in Figure 7 and the values of k_1 and k_2 maximizing the estimated system lifetime are selected.

The parameter ℓ is set for tuning the variance of MFC deterioration trajectories

$$v' = v_0/\ell, \beta' = \beta_0 \cdot \ell \quad (19)$$

where v', β' are perturbed parameters that are used as the shape and scale parameters of the Gamma process used in the simulations. The larger the value of ℓ , the higher the variance of MFC deterioration trajectories [34].

The shape and scale parameters of the random effect models (Equations (10)) are computed by

$$\delta = \frac{1}{h}, \phi = \beta_0 \ell h \quad (20)$$

where h is a constant to tune the variance of the used Gamma distribution, taken equal to 1.5 in the simulations.

Table 1: Main fuel cell parameters used in the simulation.

Parameter	Description	Value	Unit
L_{min}	Fuel cell stack minimal power	0.42	$W.cm^{-2}$
L_{nom}	Fuel cell stack nominal power	2.381	$W.cm^{-2}$
L_{max}	Fuel cell stack maximal power	3.869	$W.cm^{-2}$
$\bar{T}_{R,min}$	Expected fuel cell stack lifetime under minimal power	200	h
$\bar{T}_{R,nom}$	Expected fuel cell stack lifetime under nominal power	1788	h
$\bar{T}_{R,max}$	Expected fuel cell stack lifetime under maximal power	200	h
$\nu_{0,min}$	Shape parameter of the Gamma process model under minimal power	1.114	
$\nu_{0,nom}$	Shape parameter of the Gamma process model under nominal power	0.125	
$\nu_{0,max}$	Shape parameter of the Gamma process model under maximal power	1.114	
β_0	Fitted scale parameter of the Gamma process model	4.4×10^{-4}	
FT	Fuel cell stack failure threshold	0.278	$\Omega.cm^2$
R_0	Initial fuel cell stack resistance	0.1803	$\Omega.cm^2$
ℓ	Hyper-parameters for tuning fuel cell deterioration trajectory variance	10	
h	Hyper-parameter for setting random effect model parameters	1.5	
k_1	Hyper-parameters for the proposed EMS	15	
k_2		88	

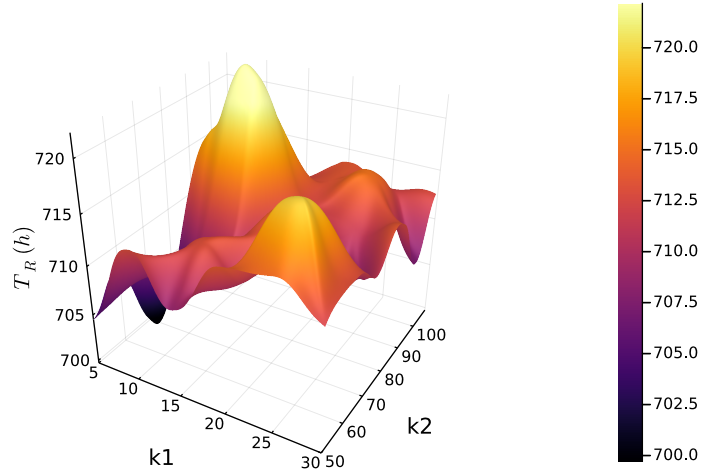


Figure 7: Selecting decision parameters k_1, k_2 . The surface stands for simulated MFC system lifetime T_R ; we select k_1, k_2 such that T_R is the highest.

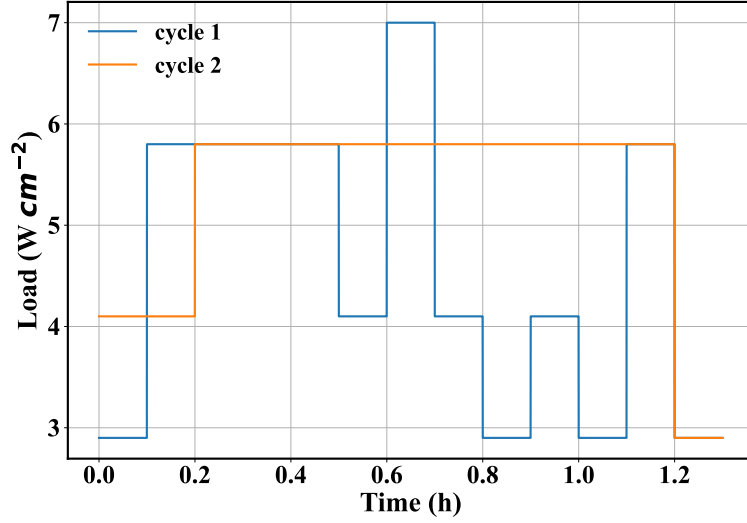


Figure 8: Realization examples of the two considered random load profiles.

The coefficients in the deterioration rate function (Equation (9)) can be calculated based on the above deterioration parameters. For instance, when $\ell = 10$, the parameters in $D(L)$ are calculated as: $A_1 = 0.0257$, $A_2 = 0.0447$, $B = 0.0124$.

The initial resistances for the three stacks are set as

$$R_{fc1}^{ini} = R_0 + \Delta R_0, \quad R_{fc2}^{ini} = R_0, \quad R_{fc3}^{ini} = R_0 \quad (21)$$

where $\Delta R_0 = 0.01 \Omega.cm^2$ is the initial increment added to FC1 to simulate an aged stack. In practice, deterioration variability exists which varies the health states of the studied stacks. Thereby, we designed this initial deterioration level difference for testing the proposed management strategy.

Random dynamic load cycle. Two Markov chain-based dynamic random cycles are considered for the numerical experiments; a realization of each of these two random load profiles is given in Figure 8. Load cycle 1 is designed to be relatively more dynamic, that is, it has a relatively smaller probability of staying at the current state compared to load cycle 2. The design of different load dynamics is accomplished by adjusting the transition probability matrix in the proposed Markov chain models. These two cycles help to assess the performance of the proposed EMSs under two different operation scenarios. The calculation of the transition state values is based both on the fuel cell stack's output power level (L_{max}) [41] and a reference fuel cell dynamic load cycle [42]. The details of these profiles refer to Appendix A.

4.2. Comparison strategies

Daisy Chain average load and deterioration-aware Daisy Chain average load strategies. The classical daisy chain and average load strategies, [43], are adapted in order to design two operation strategies that will be used for performance comparison purposes, i.e., Daisy Chain-based Average Load Strategy, and Deterioration-aware Daisy Chain Average Load Strategy sketched in Figure 9. The decision on the selected operating stacks and their operating loads are two decisions to be made in these strategies.

- Daisy Chain-based average load (DC-ave). DC-ave strategy decides the operating stacks based on the Daisy Chain strategy, i.e., sequentially switching the operating stacks. Then their operating loads are decided by the Average Load method, namely, equally distributing the load demand among the working stacks.
- Deterioration-aware Daisy Chain-based average load (DDC-ave). DDC-ave also decides the operating loads of all stacks by using the Average Load strategy. But the operating stacks are decided in a deterioration-aware

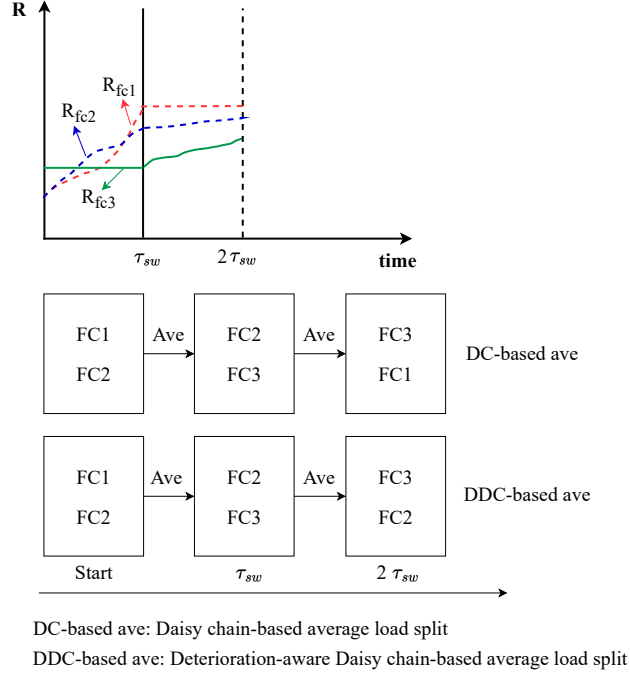


Figure 9: Basic decision process of DC-ave and DDC-ave strategies.

manner rather than the totally sequential one as in DC-ave. This deterioration-aware strategy will stop the most deteriorated stack and replace it with the previously stopped stack. In this way, the overall system deterioration is considered to be balanced in the sense that the more deteriorated stack is prevented from further deteriorating.

Parameters for DC-ave and DDC-ave strategies. The decision time interval τ_{sw} needs to be set for the DC-ave and DDC-ave strategies. Its values are investigated and optimized under deterministic scenarios in order to compare the lifetimes obtained under different parameter settings. The deterministic scenarios mean that the expected value calculates the resistance deterioration instead of random deteriorating values, and the random dynamic load cycle is kept the same for each simulation. Figure 10 shows the simulated lifetimes for a series of τ_{sw} . The DDC-ave is used as the EMS. It is seen that the overall number of start and stop times are decreasing with the increment of τ_{sw} . The maximum lifetime is observed at $\tau_{sw} = 45\text{h}$, thus it is chosen for the following simulations. Note that the lifetime drop in $\tau_{sw} = 55\text{h}$ is due to the extra deteriorations caused by the load amplitude and the load variation operation modes which result in a shorter lifetime.

4.3. Performance indicators

Lifetime-related indicators are established to assess the performance of the proposed strategy. The first indicator ($\Delta T_{R,pct}$) gives the relative improvement in lifetime compared to the average load split strategy which is computed by:

$$\Delta T_{R,pct} = \frac{\bar{T}_{R,dec} - \bar{T}_{R,ave}}{\bar{T}_{R,ave}} \times 100\% \quad (22)$$

where $\bar{T}_{R,dec}$ is the mean simulated lifetime over N trajectories that are simulated under the proposed load allocation strategy, that is $\bar{T}_{R,dec} = \frac{\sum_{i=1}^N T_{i,R,dec}}{N}$, with $T_{i,R}$ the simulated lifetime of trajectory i . $\bar{T}_{R,ave}$ is the mean simulated lifetime under the average load split policy.

The second indicator $T_{R,pct}^+$ represents, in percentage terms, the number of the simulated lifetimes under the proposed policy that are higher than those obtained with the average load split method. Let N^+ denote the number of

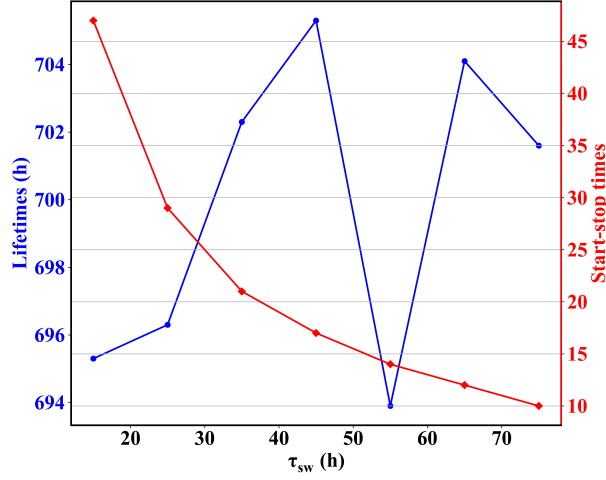


Figure 10: Simulated lifetimes and the number of start-stop events under different decision time intervals (τ_{sw}).

lifetimes obtained under the proposed load allocation decision ($T_{R,dec}$) is larger than the lifetime under the average load split policy ($T_{R,ave}$). The second proposed indicator can then be evaluated as:

$$T_{R,pct}^+ = N^+ / N \times 100\% \quad (23)$$

Due to the complexity of the obtained system lifetime distribution, it can be necessary to compare the obtained lifetimes with the mean lifetime under the average load split method ($\bar{T}_{R,ave}$). Such a comparison may offer additional information on the performance of the proposed strategy, by quantifying its ability to right-skew the lifetime distribution of the MFC system. The third performance indicator thus compares the simulated lifetimes to the mean lifetime with average load split method, which writes:

$$\begin{aligned} T_{R,pct}^{ave} &= \frac{N_{ave}^+}{N} \times 100\% \\ T_{R,pct}^{dec} &= \frac{N_{dec}^+}{N} \times 100\% \end{aligned} \quad (24)$$

where N_{ave}^+ stands for the number of lifetimes under the average load split policy that are larger than $\bar{T}_{R,ave}$. N_{dec}^+ denotes the number of the lifetime obtained under the proposed load allocation strategy that are larger than $\bar{T}_{R,ave}$.

4.4. Results for a two-stack MFC management

We first present the simulation results for the management of a two-stack MFC system: in this case, there is no switch on/off decision to make, but only the load allocation decision. First, the influence of the characteristic of the dynamic random load profiles on the performance of the proposed decision-making strategy is studied by comparing two different load cycles (load cycle 1 vs load cycle 2, see Figure 8). According to the obtained results, Monte Carlo simulations are further performed on load cycle 1 to check the average performance. Specifically, the simulations are conducted considering four types of stochastic deterioration models (GP, GP-RE, GP-RM, and GP-RV).

Optimization algorithm convergence check. A nonlinear optimization problem is formulated in the proposed decision-making strategy, thus, the solution algorithm needs to be able to handle the constrained nonlinear optimization. Besides, we have to be aware that it is time-consuming to simulate the MFC system from the beginning till system failure. Therefore, a solution algorithm with fast convergence is desired. Therefore, the Sequential least-squares programming (SLSQP) algorithm is used, [44]. SLSQP methods can solve a constrained nonlinear optimization problem in an iterative manner. The main optimization parameters for SLSQP solver are the maximum number of iterations and the precision goal for the objective function in the stopping criterion.

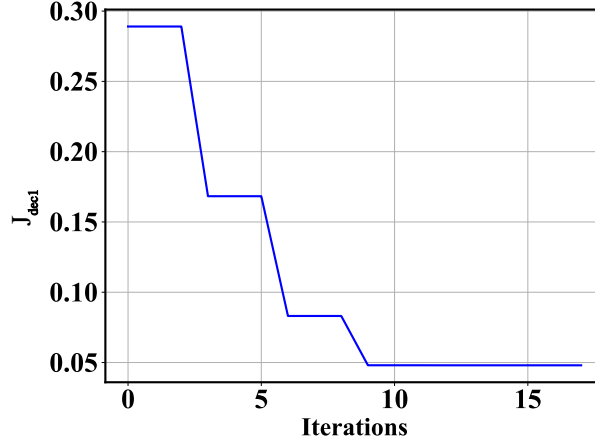


Figure 11: Convergence check of the SLSQP algorithm.

The convergence of SLSQP algorithm is investigated on the optimization of a single load allocation decision. In this optimization, the resistance values of the two stacks are set as $R_{FC1} = 0.2003 \Omega.cm^2$ and $R_{FC2} = 0.1803 \Omega.cm^2$. The power demand is defined as $5.2 W.cm^{-2}$. The maximum number of iterations of SLSQP is set at 100, and the precision goal for the objective function is set at 1×10^{-8} . These optimization solver-related parameters are set to ensure a reasonable optimization time as well as convergence. The objective function values J_{dec1} are plotted in Figure 11. It is seen that the SLSQP ensures a quick convergence after 8 evaluations (the final objective function value is 0.048). The resulting optimal load allocations are $L_{fc1} = 2.57 W.cm^{-2}$, $L_{fc2} = 2.63 W.cm^{-2}$.

Analyzing the effect of the knowledge of the load event duration and of the decision schedule on the policy performance.

- Investigating the influence of the knowledge of the event duration

Let's consider a demand profile following the random load cycle 1 (Figure 8). The expected event duration (i.e. the time until the next load change event) might be known or unknown at the decision time. If it is unknown, it can be estimated based on the MC model for all possible load levels. According to Equation (A.4) and the MC model defined in Equation (A.5), the expected event duration for four possible load demands is equal to 400s. A comparative study to investigate the load allocation policy performance when (i) the event duration is known and (ii) when it is unknown and only the expected event duration is available is performed by Monte Carlo simulations (with histories of $N = 600$). The GP and GP-RE models are selected to model fuel cell resistance deterioration (both the classic Gamma process model and random-effect models are considered). The lifetime results are summarized in Table 2. The lifetime improvement percentage ($\Delta T_{R,pct}$) in the table is calculated by:

$$\Delta T_{R,pct} = \frac{\overline{T}_{R,exact\ duration} - \overline{T}_{R,expected\ duration}}{\overline{T}_{R,expected\ duration}} \times 100\% \quad (25)$$

where $\overline{T}_{R,exact\ duration}$ represents the average lifetime simulated with a known event duration, $\overline{T}_{R,expected\ duration}$ is the average lifetime simulated without known exact event duration. $\Delta T_{R,pct}$ qualifies the value of having load profile information in terms of system lifetime improvement. A higher $\Delta T_{R,pct}$ indicates that knowing the event duration allows a significant improvement in the MFC system lifetime.

It is seen from the $\Delta T_{R,pct}$ results that for both GP and GP-RE models the lifetime improvements are relatively small. This result shows that, in the conditions of the comparative study, the proposed strategy is robust to the absence of load profile information. Not knowing the exact event duration does not entail a significant loss of the EMS strategy performance.

- Checking the influence of scheduling an extra decision

Table 2: Lifetime comparison for with and without event duration information.

Models	Event duration known		Event duration unknown		$\Delta T_{R,pct}(\%)$
	\bar{T}_R (h)	$T_{R,med}$ (h)	\bar{T}_R (h)	$T_{R,med}$ (h)	
GP	475	477	472	473	0.45
GP-RE	687	566	675	573	1.74

Table 3: Lifetime comparison for with and without scheduling extra decision - load cycle 1 (Figure 8).

Models	With extra decision		Without extra decision		$\Delta T_{R,pct}(\%)$
	\bar{T}_R (h)	$T_{R,med}$ (h)	\bar{T}_R (h)	$T_{R,med}$ (h)	
GP	476	477	475	477	0.2
GP-RE	708	608	687	566	3.15

The next step is to explore the possibilities of improving system lifetime results by scheduling an extra decision before the occurrence of the next load change event. The simulation results are compared on both load cycle 1 and load cycle 2. In Figure 8 showing two realizations of the above-defined load cycles, it can be observed that load cycle 2 is relatively less dynamic compared with load cycle 1: this is ruled by the transition matrix defined in the MC model and the probability of staying at the current state in Equation (A.6) is much larger than that in Equation (A.5). Therefore, load cycle 2 presents a relatively longer event duration. In this situation, it can be interesting to check whether it could be worthwhile to schedule an extra decision in the case where the next load change event occurs late.

We thus propose to add an extra decision to the previous event-based decision strategy when the event duration τ_e exceeds a predefined duration threshold $\tau_{e,th}$, namely, $\tau_e \geq \tau_{e,th}$. According to the simulation results, $\tau_{e,th}$ is taken as $10\tau_s$. If the event duration condition is satisfied, a decision is scheduled in the middle of the event duration. Notice that here we are assuming that the event duration τ_e is known for the current event.

The lifetime comparison results of the two load cycles are summarized in Table 3, and Table 4, respectively. The lifetime improvement percentage in the table is calculated by:

$$\Delta T_{R,pct} = \frac{\bar{T}_{R,extra\ decision} - \bar{T}_{R,no\ extra\ decision}}{\bar{T}_{R,no\ extra\ decision}} \times 100\% \quad (26)$$

where $\bar{T}_{R,extra\ decision}$ stands for the average lifetime obtained from the proposed strategy with the extra decision, and $\bar{T}_{R,no\ extra\ decision}$ is the average lifetime obtained from the event-based load allocation strategy where the decisions are scheduled at each load change event.

For the GP deterioration models, no obvious improvement is observed in both load cycles. By contrast, a relatively obvious difference is observed for the random-effect model, i.e. GP-RE. The average lifetime is improved by 3.15% when adding extra decisions under load cycle 1. This value is increased to 9.46% for load cycle 2. These results verify the efficiency of our strategy for the random-effect deterioration model. Moreover, for the load profile with a relatively long event duration, the extra decision helps to reallocate the loads among stacks to balance overall system deterioration such that an improved system life can be obtained. The GP-RE model considers the deterioration variability and their deterioration trajectories show high variability compared to the standard GP model. Thus, an obvious improvement in average system life is observed for the GP-RE model.

Monte Carlo simulation results. The performance of the proposed management strategy has been assessed using Monte Carlo simulation, with a comparison between the proposed strategy and the average load split strategy. Based on the previously obtained results in Section 4.4, it has been observed that our proposed strategy is robust to the lack of information on event duration. Thus, in this section, we focus on investigating the performance of the proposed management strategy under different deterioration models. Load cycle 1 is used as the load demand profile.

The number of required Monte Carlo simulation histories has been chosen to ensure the convergence of final simulation results. $N = 600$ is selected based on the Monte Carlo simulation results shown in Figure 12, which show

Table 4: Lifetime comparison for with and without scheduling extra decision - load cycle 2 (Figure 8).

Models	With extra decision		Without extra decision		$\Delta T_{R,pct}(\%)$
	\bar{T}_R (h)	$T_{R,med}$ (h)	\bar{T}_R (h)	$T_{R,med}$ (h)	
GP	650	651	648	647	0.35
GP-RE	1261	804	1152	742	9.46

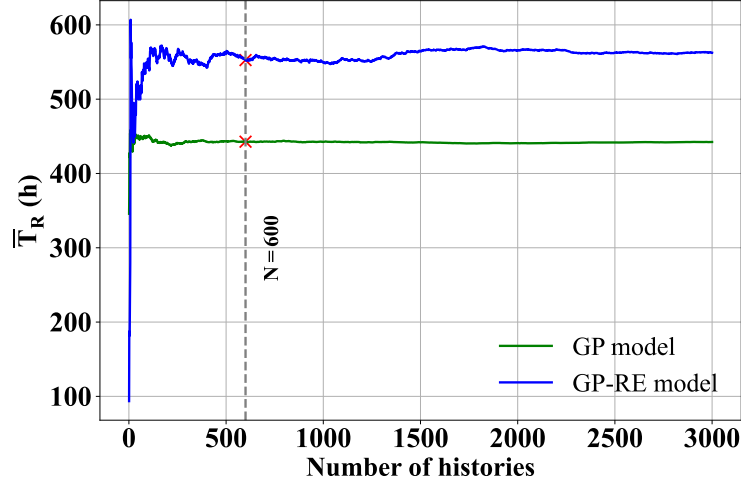


Figure 12: Convergence check for Monte Carlo simulation histories.

that convergence is guaranteed for this number of histories.

Firstly, the lifetime histograms of the different deterioration models are presented. Figure 13 shows the lifetime histogram results. In all figures, the “dec” represents the decision-making strategy (proposed method), and “ave” stands for the average load split method. By comparing the GP model results in Figure 13, it is seen that the histograms are getting wider. Regarding the shapes of the different lifetime histograms obtained for the deterioration models, the GP, and GP-RV models are approximately Gaussian (symmetrically) distributed, whereas the GP-RE and GP-RM models are not symmetrically distributed.

The corresponding cumulative distribution function results are plotted in Figure 14. The failure probability (F_x) taken from Monte Carlo analysis is shown in these cumulative distribution function (CDF) curves. In the CDF curve results for the GP model, it is seen that the MFC system reaches the value $F_{0.1}$ (i.e. failure probability at 0.1) at approximately 317.5h for the average load strategy. On the other hand, when the system operates with load allocation decision (our strategy), the system attains $F_{0.1}$ at approximately 352.2h, resulting in a meaningful prolongation of system life. Similar improvements are observed for the three random-effect models.

The five lifetime-related indicators, i.e., mean system lifetime \bar{T}_R , median system lifetime $T_{R,med}$, and four lifetimes comparison percentages ($\Delta T_{R,pct}$, $T_{R,pct}^+$, $T_{R,pct}^{ave}$, $T_{R,pct}^{dec}$) are computed from the obtained simulation results. Table 5 summarizes the results of the indicators. For all cases, the lifetimes (both the mean and median) obtained from load allocation decisions are larger than that of the average split strategy. These results are also visible with the average lifetime improvement indicator $\Delta T_{R,pct}$. The values of $T_{R,pct}^+$ show that generally over 60% of the simulated lifetimes are higher than the ones resulting from the implementation of the average load split method. Moreover, the comparison of the lifetimes of the proposed decision strategy and the average split strategy indicates that our strategy can achieve around 20% of lifetime improvement.

By comparing the results with the GP model to the random effects models, it is observed that the average lifetime improvement indicator $\Delta T_{R,pct}$ is improved. These results confirm that when considering the stack deterioration heterogeneity, the proposed load allocation strategy can still obtain an improved system lifetime compared with the

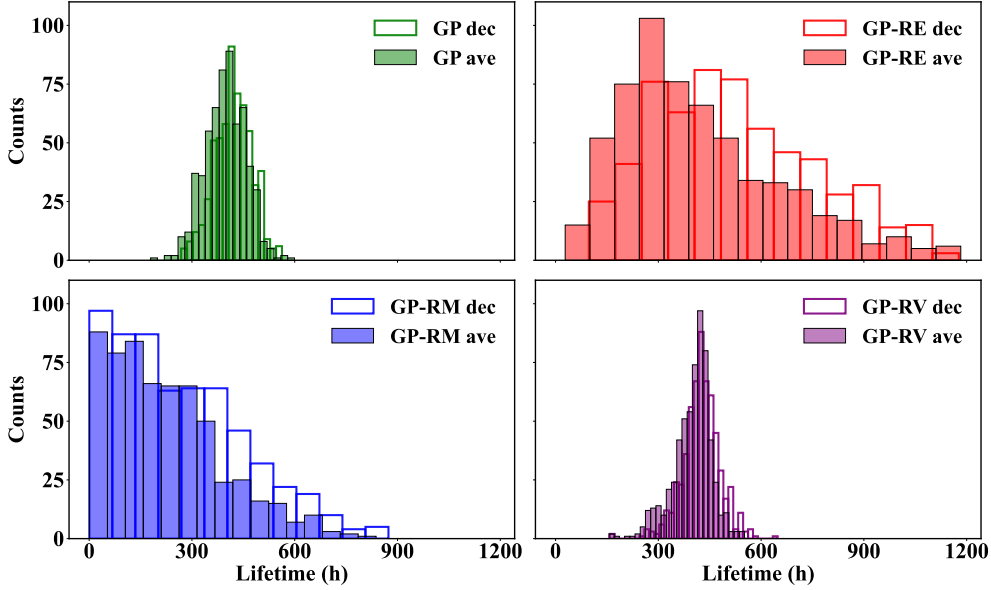


Figure 13: Histograms of the simulated lifetimes: compare our strategy with average load split.

Table 5: Lifetime indicator results for $\ell = 10$

	\bar{T}_R (h)		$T_{R,med}$ (h)		$\Delta T_{R,pct}$ (%)	$T_{R,pct}^+$ (%)	$T_{R,pct}^{ave}$ (%)	$T_{R,pct}^{dec}$ (%)
	ave	dec	ave	dec				
GP	397	420	399	421	5.8	64.0	51.5	68.7
GP-RE	421	525	368	492	24.6	63.5	40.3	64.5
GP-RM	225	266	199	234	18.5	55.5	44.2	50.7
GP-RV	399	426	410	426	6.1	61.3	58.2	73.0

classical average split strategy. For the random effect-based models, the statistical information of the studied stochastic models is used in the decision-making procedure to decide the optimal load allocations. In the GP deterioration model, the deterioration behavior of different stacks tends to be similar on average, and the statistical information may not contribute too much to improving fuel cell lifetime. On the contrary, the variability of individual stack deterioration behavior is highlighted in random effects models, thus it would be useful to include the statistical information when computing the optimal load allocations. These are reflected by the average lifetime improvement indicator $\Delta T_{R,pct}$ where the results of the random effects models are generally better than those of the GP models. However, the random effects increase the variability of the first hitting time, and the indicators of $T_{R,pct}^+$, $T_{R,pct}^{ave}$, and $T_{R,pct}^{dec}$ are slightly lower than those of the GP model. However, the global results with the decision-making strategy are better than those for the comparison strategy, i.e., the average load split method.

4.5. Results for the three-stack management problem

This section presents the results of the three stacks operation problem with start and stop events using the two-step management strategy.

Deterministic one-run simulation results. To understand and compare the behavior of the studied EMSs, the deterioration trajectories under deterministic settings are investigated for all management strategies. The load profile imposed on the studied MFC system and fuel cell deterioration is thus set to be deterministic, such that the MFC deterioration results are comparable for different EMSs.

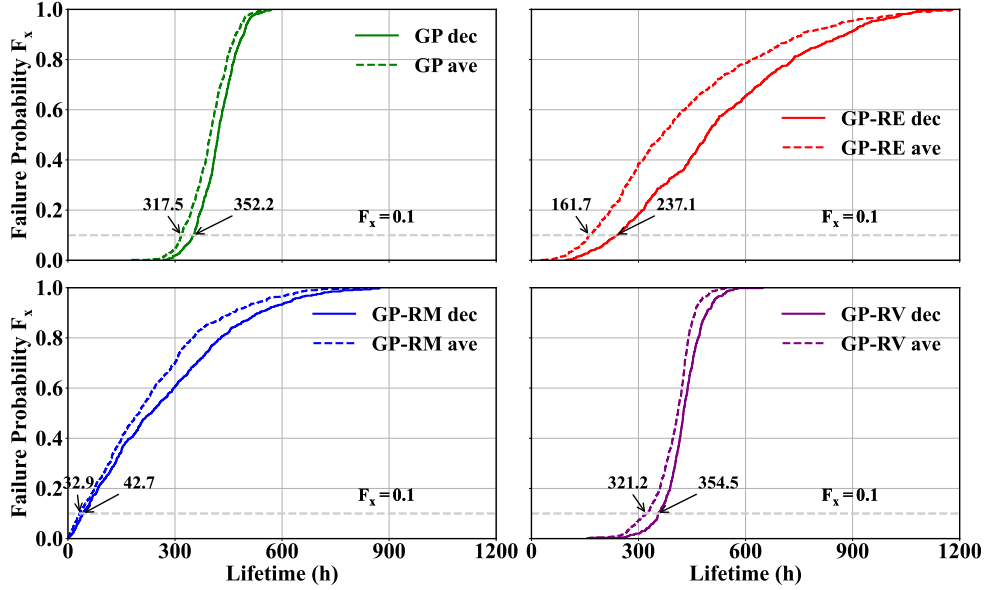


Figure 14: CDF comparison results.

Three independent simulations are performed from the beginning of life till system failure, obtaining three one-run trajectories. Figures 15, 16, and 17 show the detailed resistance deterioration level and load allocations information at each switching decision (here the switching decision specifically refers to switch on/off different stacks). For the studied MFC system, the deterioration variability is modeled by a GP-RE model as introduced in the parameter setting section. As a result, each stack is assigned with (sampled from a Gamma law) a different scale parameter β to simulate this random effect. For instance, in the trajectory results as shown in Figure 15, FC3 is assigned with the biggest scale parameter $\beta_{FC_3} = 3.67 \times 10^{-3}$. This is why FC3 shows the highest deterioration rates. The scale parameters used in the simulation of DDC-ave and our strategies are specified in the figure captions of Figures 16 & 17.

Our strategy obtained the highest lifetime for the studied system, 1731.2h, followed by the DDC-ave strategy 1641h, and the DC-ave strategy procedures the lowest lifetime 1467.8h. DC-ave is a pure sequential switching strategy for deciding the operating stacks without considering stacks deterioration information. This can be observed from Figure 15, the three stacks are switched on/off in sequential order: {FC2 off, FC1, FC3 on} \rightarrow {FC1 off, FC2, FC3 on} \rightarrow {FC3 off, FC1, FC2 on} \dots . By contrast, the deterioration-aware strategies decide the switching actions by taking into account system deterioration states. This is beneficial for balancing the deterioration levels of all stacks so that the overall system life can be extended. It is observed that in DDC-ave and our strategy, they switch off FC1 in the first decision, then for the remaining decisions, they keep FC1 running, only switching between FC2 and FC3. This is due to FC1 being the most deteriorated stack at the beginning of life, thus it is beneficial to stop it in the first decision. In the following decisions, it will be restarted when the switch decision criterion is satisfied.

It is observed from the results (Figures 15, 16, and 17) that the three resistance trajectories are gradually grouped together from DC-ave strategy to DDC-ave strategy, and finally our strategy. Figure 18 shows the comparison results of our strategy to two comparison strategies. Our strategy obtains the largest lifetime and the resistance values at the end of life are close to each other, while the comparison strategies fail to balance overall deterioration. These results show that the proposed strategy can effectively control the deterioration variability among different stacks which helps to balance overall system deterioration levels, thus achieving an improved system lifetime.

Monte Carlo simulation results. The overall simulated lifetimes are summarized in Figure 19(a). The lifetime-related indicators are calculated based on this histogram and listed in Table 6. For the lifetime improvement percentage result, we have computed the values for our decision-making strategy with respect to the DC-ave and DDC-ave strategies, respectively. Then the percentage values ($T_{R,pct}^{DC}$, $T_{R,pct}^{DDC}$, and $T_{R,pct}^{dec}$) of the Monte Carlo simulation lifetimes that are larger than the average lifetime of the DC-ave strategy for all studied strategies, namely, the DC-ave, DDC-

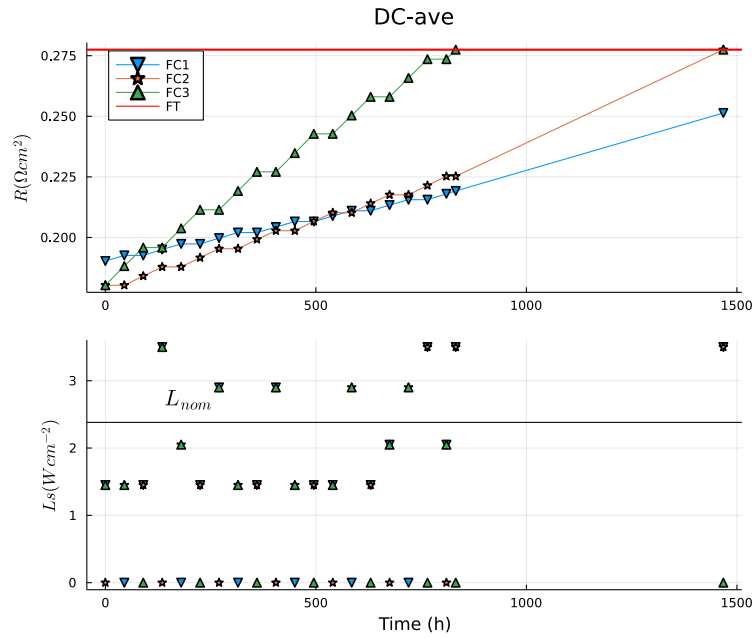


Figure 15: Switch decisions results for DC-ave strategy (deterministic scenario, $\beta_{FC1} = 1.067 \times 10^{-4}$, $\beta_{FC2} = 1.039 \times 10^{-3}$, $\beta_{FC3} = 3.67 \times 10^{-3}$).

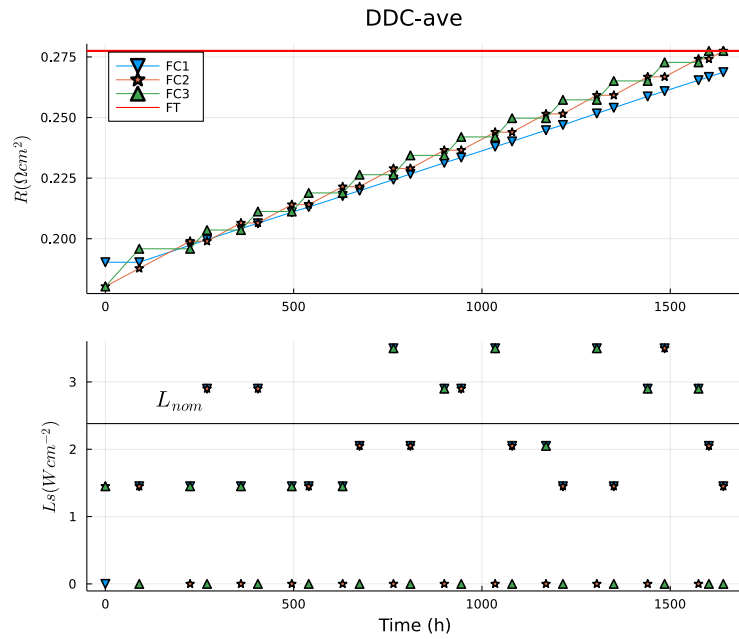


Figure 16: Switch decisions results for DDC-ave strategy (deterministic scenario, $\beta_{FC1} = 1.067 \times 10^{-4}$, $\beta_{FC2} = 1.039 \times 10^{-3}$, $\beta_{FC3} = 3.67 \times 10^{-3}$).

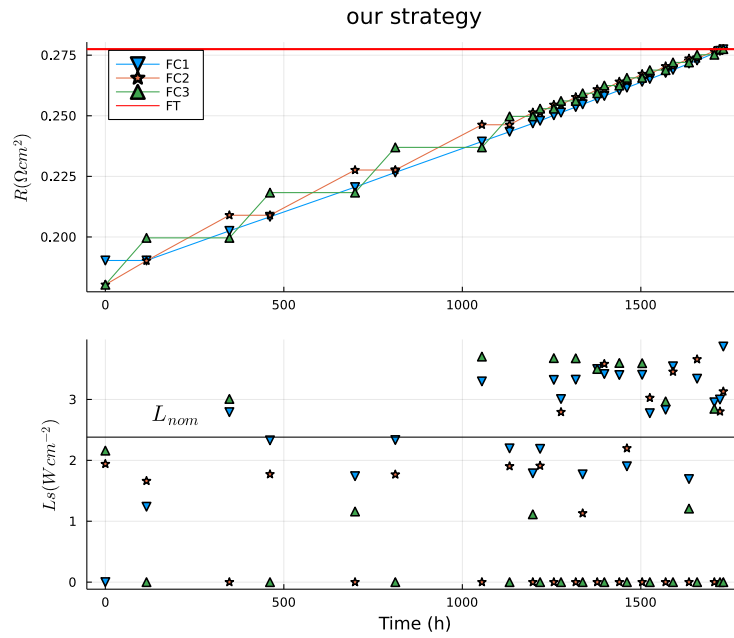


Figure 17: Switch decisions results for our strategy (deterministic scenario, $\beta_{FC1} = 1.067 \times 10^{-4}$, $\beta_{FC2} = 1.039 \times 10^{-3}$, $\beta_{FC3} = 3.67 \times 10^{-3}$).

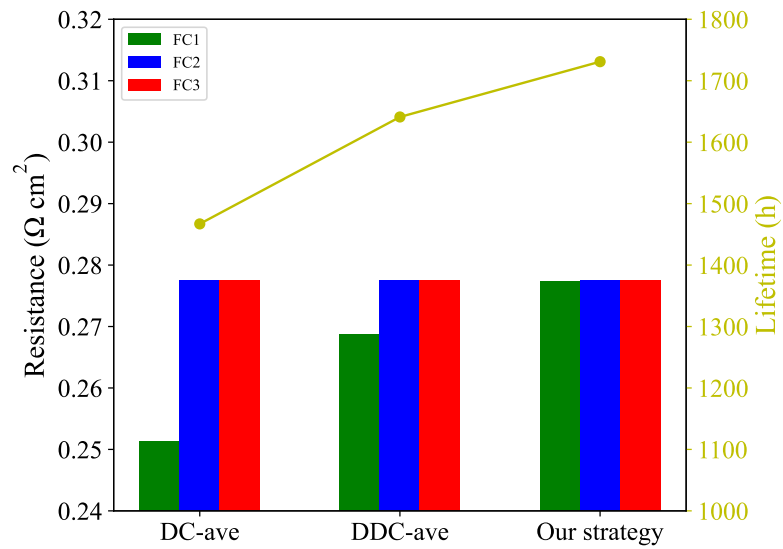


Figure 18: Resistance and system lifetime comparison results for proposed strategy and two comparison strategies.

Table 6: Overall lifetime indexes results.

	$\Delta T_{R,pct}(\%)$	$\Delta T_{R,pct}(\%)$	$T_{R,pct}^{DC}(\%)$	$T_{R,pct}^{DDC}(\%)$	$T_{R,pct}^{dec}(\%)$
	DC-ave	DDC-ave			
	Our strategy	Our strategy			
$\ell = 10$	21.7	8.1	45	51	61

ave, and proposed decision-making strategy. Among the three studied strategies, our strategy obtained the highest lifetime ($\bar{T}_R = 1268h$, $T_{R,med} = 1229h$). The mean and median lifetimes of the DDC-ave strategy are $1127h$ and $1062h$, respectively. The DC-ave strategy only obtains an average lifetime of $1042h$ and a median lifetime of $957h$. Compared with the DC-ave strategy, our approach obtains 21.7% of average lifetime improvement. In comparison to the deterioration-aware strategy (DDC-ave), our strategy helps to improve the average system lifetime by 8.1%. 45% of simulated lifetimes by DC-ave are larger than the average lifetime of the DC-ave strategy. For the deterioration-aware DC-ave strategy, this percentage increased to 51%. Our strategy further improves this value to 61%. Thus, the proposed strategy outperforms both the basic daisy chain-based (deterioration-unaware) and deterioration-aware strategies.

Figure 19(b) plots the CDF curves based on the histogram results shown in Figure 19(a). The CDF results confirm the above conclusion. The proposed strategy greatly lowers the system failure probabilities in short-lifetime range shown in the figure, thus obtaining an extended system lifetime.

Due to the stochastic deterioration behavior, it is shown that the relevance of the proposed energy management strategy can only be established through a huge number (greater than 1000) of run-to-failure trails. This is nevertheless not practically realizable for the studied multi-stack fuel cell system. Therefore, at this stage of study, we are focusing on assessing the efficiency of the proposed deterioration-aware EMS through simulations.

The proposed energy management strategy can be applied to other oversized multi-stack fuel cell systems with different sizes and power levels. Regarding the size of the system, the proposed strategy is introduced for N_s stacks with n operating stacks ($n \leq N_s$). Both the load allocation decisions and the switching decisions can be obtained for different N_s and n . Regarding the power level of the system, the proposed strategy can be applied to other multi-stack fuel cell systems with different power levels when the relative deterioration data is available.

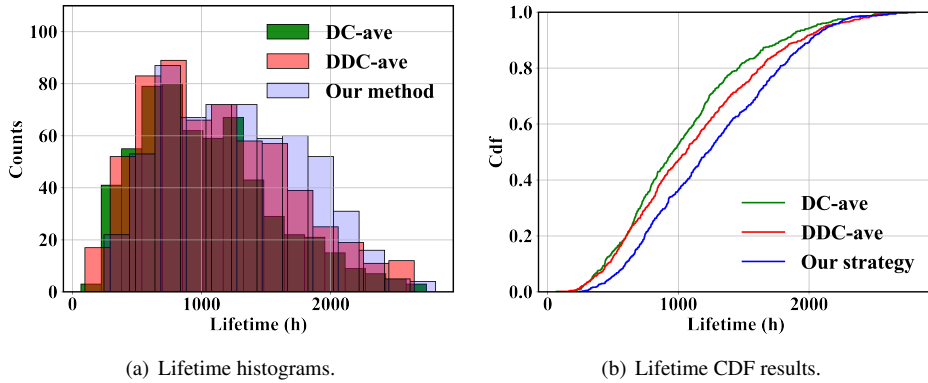


Figure 19: Simulation results for random effects model under random load profile.

5. Conclusion

This paper studied the energy management problem of an oversized MFC system under random dynamic load profiles. First, a non-homogeneous Gamma process-based deterioration model is used to capture the load-dependency and stack-to-stack deterioration variability of the studied MFC. The stack deterioration rate is expressed as an empirical function of its operating load, making the deterioration load-dependent. Regarding the deterioration variability, a

random effect is added to the Gamma process model on its scale parameter, taken as a random variable following a Gamma law. Next, a two-step decision-making strategy is proposed for deciding optimal load allocation for operating stacks and switching decisions for selecting the operating stacks. The strategy for deciding the load allocations is validated on a two-stack fuel cell system, achieving a maximum lifetime improvement of 24.6% compared to the average load split strategy. Then, the operation of an oversized three-stack fuel cell is managed by adding a switching decision. The Monte Carlo simulation results confirmed an average lifetime improvement of 21.7% compared to the DC-ave strategy and 8.1% compared to the DDC-ave strategy. From the obtained simulation results, the following conclusions were made:

- 1) Stochastic processes like the Gamma process are promising tools for adapting to MFC deterioration modeling.
- 2) The proposed decision-making strategy shows an example of prolonging MFC system lifetime when exposed to randomness in both fuel cell deterioration and operating loads.
- 3) Higher lifetime is obtained when there is deterioration variability between stacks which highlights the potential of using such EMS for MFC system.

In the following work, experimental works will be conducted on the studied MFC system to collect the deterioration data for constructing the MFC deterioration model; and further, validate the proposed strategy. Efforts will also be made on developing a maintenance-based EMS by integrating stack replacement scheduling into the proposed strategy.

Declaration of Competing interest

The authors declare that they have no known competing financial interests or personal relationships that could be appeared to influence the work reported in this paper.

Acknowledgments

This work has been partially supported by the ANR project ANR-15-IDEX-02 and MIAI@Grenoble Alpes (ANR-19-P31A-0003)

Appendix A. Markov Chain-based random dynamic load cycle

A discrete Markov Chain (MC) model is used to construct the random dynamic load profile. Let S denote a (finite) set of possible power demands with c elements $\{x_1, \dots, x_c\}$. The set S is called the state space, and x_1, \dots, x_c are the state values. The stochastic sequence of X_t (with discrete time t) of the successive power demands (taken in S) can be modeled by a Markov Chain if it satisfies the Markov property, which is expressed as (memorylessness property):

$$P\{X_{t+1} = y | X_t, X_{t-1}, \dots\} = P\{X_{t+1} = y | X_t\} \quad (\text{A.1})$$

where $P(\cdot)$ denotes the probability of the event. The future behavior of the process does not depend on its past but only on its present state. The dynamics of a MC model is fully determined by a set of transition probabilities:

$$P(x, y) = P(X_{t+1} = y | X_t = x) \quad (x, y \in S) \quad (\text{A.2})$$

where $P(x, y)$ is the transition probability from state x to state y in one step. $P(x, \cdot)$ is the conditional distribution of X_{t+1} given $X_t = x$. The transition probabilities between the different states can be arranged in a Markov matrix P_c where

$$P_{i,j} = P(x_i, x_j) \quad 1 \leq i, j \leq n \quad (\text{A.3})$$

and P_c satisfies:

- each element of P_c is non-negative, and
- each row of P_c sums to 1.

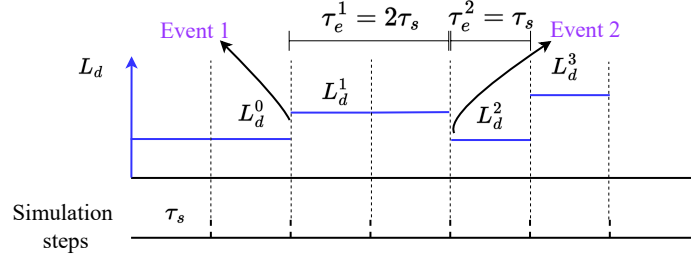


Figure A.1: Schematic diagram of generating random load profile.

For simulation purposes, the MC model can be used to generate a random power demand profile X_t as follows:

- Draw an initial state X_0 from a specified initial distribution.
- For each $t = 0, 1, \dots$, draw X_{t+1} from the transition probability matrix $P(x, y)$.

Assuming that the load profile imposed to the MFC system $L_d(t)$ can be described as an MC model with Markov transition matrix P_{tr} and all possible states L_{ds} , we can generate random dynamic load profiles for MFC systems. At each simulation step τ_s (equivalent to the discrete time step t defined in Equation (A.1)), the next state is drawn from transition probability matrix $P(x, y)$. In the case of deterministic power demands, the duration of a load change event (τ_e) is fixed, however, this is not the case in random load profiles. For the random load profile, the load demand level of each simulation step τ_s is generated through a Markov Chain model, thus, the load change event duration varies from time to time. This is illustrated in Figure A.1 as the event duration of Event 1 is $2\tau_s$ whereas the duration of the following event equals τ_s .

The expected duration of current event $\bar{\tau}_e$ is computed by (Assuming we are at decision k , and the load demand levels $L_d^k, L_d^k \in L_{ds}$ are known exactly):

$$\begin{aligned} \bar{\tau}_e &= \sum_{i=0}^{\infty} \tau_s(i+1)P^i(1-P) \\ &= \tau_s \frac{1}{1-P} \end{aligned} \quad (\text{A.4})$$

where τ_s is the discrete simulation time step used in the Markov Chain model. P is the probability of staying at L_d^k which is defined in P_{tr} .

Two typical dynamic load cycles are designed to investigate their influences on the performance of the proposed energy management strategy. Load cycle 1 is designed with a more frequent load change:

$$\mathbf{P}_{tr} = \begin{bmatrix} 0.1 & 0.35 & 0.35 & 0.2 \\ 0.35 & 0.1 & 0.35 & 0.2 \\ 0.2 & 0.35 & 0.1 & 0.35 \\ 0.2 & 0.35 & 0.35 & 0.1 \end{bmatrix}, L_{ds} = [2.9, 4.1, 5.8, 7.0] \quad (\text{A.5})$$

and a more static (slow load change) load profile (load cycle 2) is modeled by

$$\mathbf{P}_{tr} = \begin{bmatrix} 0.7 & 0.1 & 0.15 & 0.05 \\ 0.05 & 0.8 & 0.05 & 0.1 \\ 0.05 & 0.05 & 0.85 & 0.05 \\ 0.05 & 0.15 & 0.2 & 0.6 \end{bmatrix}, L_{ds} = [2.9, 4.1, 5.8, 7.0] \quad (\text{A.6})$$

Appendix B. Fuel cell stack operation conditions

The stack structure and operating conditions are based on the data provided in IEEE PHM 2014 data challenge [41]. The specific parameters are summarized in Table B.1.

Table B.1: Fuel cell stack structure and operating conditions

Parameter	Values/control range
Number of cells	5
Cell active area	100 cm ²
Cooling temperature	20 °C to 80 °C
Cooling flow	0 to 10 l/min
Gas temperature	20 °C to 80 °C
Gas humidification	0 to 100% RH
Air flow	1 to 100 l/min
H2 flow	0 to 30 l/min
Gas pressure	0 to 2 bars

References

- [1] Y. Hu, X. Miao, Y. Si, E. Pan, E. Zio, Prognostics and health management: A review from the perspectives of design, development and decision, *Reliability Engineering & System Safety* 217 (2022) 108063.
- [2] E. Zio, Prognostics and health management (PHM): Where are we and where do we (need to) go in theory and practice, *Reliability Engineering & System Safety* 218 (2022) 108119.
- [3] S. Dirkes, J. Leidig, P. Fisch, S. Pischinger, Prescriptive lifetime management for PEM fuel cell systems in transportation applications, part i: State of the art and conceptual design, *Energy Conversion and Management* 277 (2023) 116598.
- [4] C. Wang, M. Dou, Z. Li, R. Outbib, D. Zhao, J. Zuo, Y. Wang, B. Liang, P. Wang, Data-driven prognostics based on time-frequency analysis and symbolic recurrent neural network for fuel cells under dynamic load, *Reliability Engineering & System Safety* 233 (2023) 109123.
- [5] X. Zhao, L. Wang, Y. Zhou, B. Pan, R. Wang, L. Wang, X. Yan, Energy management strategies for fuel cell hybrid electric vehicles: Classification, comparison, and outlook, *Energy Conversion and Management* 270 (2022) 116179.
- [6] J. Desantes, R. Novella, B. Pla, M. Lopez-Juarez, Effect of dynamic and operational restrictions in the energy management strategy on fuel cell range extender electric vehicle performance and durability in driving conditions, *Energy Conversion and Management* 266 (2022) 115821.
- [7] M. Kandidayeni, M. Soleymani, A. Macias, J. P. Trovão, L. Boulon, Online power and efficiency estimation of a fuel cell system for adaptive energy management designs, *Energy Conversion and Management* 255 (2022) 115324.
- [8] M. Kandidayeni, J. Trovão, M. Soleymani, L. Boulon, Towards health-aware energy management strategies in fuel cell hybrid electric vehicles: A review, *International Journal of Hydrogen Energy* (2022).
- [9] C. Lorenzo, D. Bouquain, S. Hibon, D. Hissel, Synthesis of degradation mechanisms and of their impacts on degradation rates on proton-exchange membrane fuel cells and lithium-ion nickel–manganese–cobalt batteries in hybrid transport applications, *Reliability Engineering & System Safety* 212 (2021) 107369.
- [10] L. De Pascali, F. Biral, S. Onori, Aging-aware optimal energy management control for a parallel hybrid vehicle based on electrochemical-degradation dynamics, *IEEE Transactions on Vehicular Technology* 69 (2020) 10868–10878.
- [11] C. Tsoumpris, G. Theotokatos, A decision-making approach for the health-aware energy management of ship hybrid power plants, *Reliability Engineering & System Safety* (2023) 109263.
- [12] F. Peng, X. Xie, K. Wu, Y. Zhao, L. Ren, Online hierarchical energy management strategy for fuel cell based heavy-duty hybrid power systems aiming at collaborative performance enhancement, *Energy Conversion and Management* 276 (2023) 116501.
- [13] C. Zhang, Y. Zhang, Z. Huang, C. Lv, D. Hao, C. Liang, C. Deng, J. Chen, Real-time optimization of energy management strategy for fuel cell vehicles using inflated 3D Inception Long Short-term Memory Network-based speed prediction, *IEEE Transactions on Vehicular Technology* 70 (2021) 1190–1199.
- [14] M. Rausand, A. Hoyland, *System reliability theory: models, statistical methods, and applications*, volume 396, John Wiley & Sons, 2003.
- [15] A. Vasilyev, J. Andrews, S. J. Dunnett, L. M. Jackson, Dynamic reliability assessment of PEM fuel cell systems, *Reliability Engineering & System Safety* 210 (2021) 107539.
- [16] M. Z. Gargari, M. T. Hagh, S. G. Zadeh, Preventive maintenance scheduling of multi energy microgrid to enhance the resiliency of system, *Energy* 221 (2021) 119782.
- [17] S. Zhou, L. Fan, G. Zhang, J. Gao, Y. Lu, P. Zhao, C. Wen, L. Shi, Z. Hu, A review on proton exchange membrane multi-stack fuel cell systems: architecture, performance, and power management, *Applied Energy* 310 (2022) 118555.
- [18] N. Marx, J. Cardozo, L. Boulon, F. Gustin, D. Hissel, K. Agbossou, Comparison of the series and parallel architectures for hybrid multi-stack fuel cell-battery systems, in: *2015 IEEE Vehicle Power and Propulsion Conference (VPPC)*, IEEE, 2015, pp. 1–6.
- [19] N. Marx, D. Hissel, F. Gustin, L. Boulon, K. Agbossou, On the sizing and energy management of an hybrid multistack fuel cell–battery system for automotive applications, *International Journal of Hydrogen Energy* 42 (2017) 1518–1526.
- [20] T. Wang, Q. Li, L. Yin, W. Chen, Hydrogen consumption minimization method based on the online identification for multi-stack PEMFCs system, *International Journal of Hydrogen Energy* 44 (2019) 5074–5081.
- [21] M. Moghadari, M. Kandidayeni, L. Boulon, H. Chaoui, Hydrogen minimization of a hybrid multi-stack fuel cell vehicle using an optimization-based strategy, in: *2021 IEEE Vehicle Power and Propulsion Conference (VPPC)*, IEEE, 2021, pp. 1–5.

- [22] Y. Wang, W. Chen, A. Guo, X. Shen, Two-level energy management strategy for a hybrid power system based multi-stack fuel cell, in: ICRT 2021, American Society of Civil Engineers Reston, VA, 2022, pp. 545–556.
- [23] R. Ghaderi, M. Kandidayeni, L. Boulon, J. P. Trovão, Quadratic programming based energy management in a multi-stack fuel cell hybrid electric vehicle, in: 2021 IEEE Vehicle Power and Propulsion Conference (VPPC), IEEE, 2021, pp. 1–6.
- [24] A. M. Fernandez, M. Kandidayeni, L. Boulon, H. Chaoui, An adaptive state machine based energy management strategy for a multi-stack fuel cell hybrid electric vehicle, *IEEE Transactions on Vehicular Technology* 69 (2019) 220–234.
- [25] N. Herr, J.-M. Nicod, C. Varnier, L. Jardin, A. Sorrentino, D. Hissel, M.-C. Péra, Decision process to manage useful life of multi-stacks fuel cell systems under service constraint, *Renewable energy* 105 (2017) 590–600.
- [26] S. Zhou, G. Zhang, L. Fan, J. Gao, F. Pei, Scenario-oriented stacks allocation optimization for multi-stack fuel cell systems, *Applied Energy* 308 (2022) 118328.
- [27] W. R. Bankati, A. Macias, M. Soleymani, L. Boulon, S. Jemei, An online energy management strategy for multi-fuel cell stacks systems using remaining useful life prognostic, in: 2022 IEEE Vehicle Power and Propulsion Conference (VPPC), 2022, pp. 1–6. doi:10.1109/VPPC55846.2022.10003469.
- [28] K. W. E. Colombo, P. Schütz, V. V. Kharton, Reliability analysis for a multi-stack solid oxide fuel cell system subject to operation condition-dependent degradation, *Journal of Quality in Maintenance Engineering* (2020).
- [29] K. W. E. Colombo, V. V. Kharton, Reliability analysis of a multi-stack solid oxide fuel cell from a systems engineering perspective, *Chemical Engineering Science* 238 (2021) 116571.
- [30] S. Phommixay, M. L. Doumbia, Q. Cui, Real time power sharing of fuel cells microgrid considering short term preventive maintenance outage, in: 2019 IEEE 2nd International Conference on Renewable Energy and Power Engineering (REPE), IEEE, 2019, pp. 83–89.
- [31] J. Kim, S.-M. Lee, S. Srinivasan, C. E. Chamberlin, Modeling of Proton Exchange Membrane Fuel Cell performance with an empirical equation, *Journal of the electrochemical society* 142 (1995) 2670.
- [32] B. M. Wilamowski, H. Yu, Improved computation for levenberg–marquardt training, *IEEE transactions on neural networks* 21 (2010) 930–937.
- [33] J. Zuo, C. Cadet, Z. Li, C. Berenguer, R. Outbib, Post-prognostics decision-making strategy for load allocation on a stochastically deteriorating multi-stack fuel cell system, *Proceedings of the Institution of Mechanical Engineers, Part O: Journal of Risk and Reliability* 237 (2023) 40–57.
- [34] J. Zuo, C. Cadet, Z. Li, C. Berenguer, R. Outbib, Fuel cell stochastic deterioration modeling for energy management in a multi-stack system, in: 2022 13th International Conference on Reliability, Maintainability, and Safety (ICRMS), 2022, pp. 104–108. doi:10.1109/ICRMS55680.2022.9944566.
- [35] P. Pei, Q. Chang, T. Tang, A quick evaluating method for automotive fuel cell lifetime, *International Journal of Hydrogen Energy* 33 (2008) 3829–3836.
- [36] J. M. van Noordwijk, A survey of the application of Gamma processes in maintenance, *Reliability Engineering & System Safety* 94 (2009) 2–21.
- [37] M. B. Salem, M. Fouladirad, E. Deloux, Variance gamma process as degradation model for prognosis and imperfect maintenance of centrifugal pumps, *Reliability Engineering & System Safety* 223 (2022) 108417.
- [38] B. Wu, D. Ding, A gamma process based model for systems subject to multiple dependent competing failure processes under markovian environments, *Reliability Engineering & System Safety* 217 (2022) 108112.
- [39] K. Song, L. Cui, A common random effect induced bivariate gamma degradation process with application to remaining useful life prediction, *Reliability Engineering & System Safety* 219 (2022) 108200.
- [40] J. Zuo, C. Cadet, Z. Li, C. Bérenguer, R. Outbib, A load allocation strategy for stochastically deteriorating multi-stack PEM fuel cells, in: 32nd European Conference on Safety and Reliability (ESREL 2022), ESREL 2022, 2022, pp. 1204–1211.
- [41] R. Gouriveau, M. Hilairat, D. Hissel, S. Jemei, M. Jouin, E. Lechartier, S. Morando, E. Pahon, M. Pera, N. Zerhouni, IEEE PHM 2014 data challenge: Outline, experiments, scoring of results, winners, IEEE 2014 PHM Challenge, Tech. Rep (2014).
- [42] G. Tsoitridis, A. Pilenga, G. De Marco, T. Malkow, et al., EU harmonised test protocols for PEMFC MEA testing in single cell configuration for automotive applications, JRC Science for Policy report 27632 (2015) 21–23.
- [43] A. Khalatbarisoltani, M. Kandidayeni, L. Boulon, X. Hu, Power allocation strategy based on decentralized convex optimization in modular fuel cell systems for vehicular applications, *IEEE Transactions on Vehicular Technology* 69 (2020) 14563–14574.
- [44] J. Xie, H. Zhang, Y. Shen, M. Li, Energy consumption optimization of central air-conditioning based on sequential-least-square-programming, in: 2020 Chinese Control And Decision Conference (CCDC), IEEE, 2020, pp. 5147–5152.